THE JOURNAL OF BIOLOGICAL CHEMISTRY VOL. 291, NO. 50, pp. 26045–26055, December 9, 2016

Extension of Health Span and Life Span in *Drosophila* by S107 Requires the *calstabin* Homologue *FK506-BP2**

Received for publication, September 15, 2016, and in revised form, October 28, 2016 Published, JBC Papers in Press, November 1, 2016, DOI 10.1074/jbc.M116.758839

Tabita Kreko-Pierce, Jorge Azpurua, Rebekah E. Mahoney, and Benjamin A. Eaton[1]

From the Department of Integrative and Cellular Physiology, University of Texas Health Sciences Center at San Antonio, San Antonio, Texas 78229

Edited by Jeffrey Pessin

The accumulation of oxidative damage is strongly linked to age-dependent declines in cell function, but the contribution of oxidative damage to morbidity is still debated. Many organisms seem to tolerate oxidative damage, and the extension of health span and life span by augmenting antioxidant activity has been inconsistent. Here we use the *Drosophila* model system to investigate the relationship among oxidative stress, health span, and life span. The oxidation-dependent dissociation of the Calstabin protein from the ryanodine receptor has been shown to result in reduced muscle function in mammals. The S107 molecule is able to reestablish this binding resulting in improved muscle function. We find that S107 is able to restore motor function in aging *Drosophila* to young levels, and this effect of S107 is absent in *calstabin* (*FK506-BP2*) mutants. Interestingly, *FK506-BP2* mutant flies have reduced sensitivity to the effects of age and oxidative stress on motor function between 7 and 35 days of age. Muscle expression of FK506-BP2 in *FK506-BP2* mutants completely restores the sensitivity of motor function to both age and oxidative stress, supporting the idea that the age-dependent decline in motor function in *Drosophila* requires FK506-BP2 function within the muscle. Although *FK506-BP2* mutant flies are found to have less sensitivity to oxidative stress, *FK506-BP2* mutants do not live longer than wild type. These results demonstrate that the deleterious effects of oxidation on motor function early in life are the result of a singular event that does not compromise survival.

The oxidative stress theory of aging proposes that a critical mechanism underlying the aging process is the production of oxidants during aerobic metabolism. These reactive oxygen species can oxidize proteins, resulting in the age-dependent accumulation of oxidized macromolecules that ultimately compromise cell and organ function leading to reduced life span (1). Although it is clear from numerous studies that the products of oxidation do accumulate with age and can alter normal protein function, evidence that oxidative stress directly contributes to limiting life span is controversial (2–5). For example, a large number of studies from a diverse array of model organisms have demonstrated that experimentally compromising antioxidant pathways results in enhanced susceptibility to stress and premature reduction in cellular function, but only in some cases does it affect life span (4, 6–11). However, the converse manipulation of genetically or pharmacologically increasing antioxidant levels has resulted in only sporadic effects on health span and life span (4, 11–20). Furthermore, some long-lived bird and animal species exist with relatively high levels of oxidative stress and/or low levels of antioxidants throughout life, suggesting that these organisms are resistant to effects of oxidative stress (5, 21–25). Finally, low levels of oxidative stress can result in the induction of cytoprotective processes, resulting in enhanced protection against the effects of age on cellular function, supporting the idea that some protein oxidation events are actually beneficial for survival (2, 26, 27). It is expected that a better understanding of the molecular mechanisms underlying the effects of oxidative stress on health span and life span will help to resolve these discrepancies.

The term "health span" refers to the ages that define the optimal health of the organism. A major determinant of health span in many organisms (including humans) is the age-dependent decline in muscle function. The ryanodine receptor (RyR)[2] has been established as an important target of oxidation in aging skeletal muscle in mammals (3–5, 28, 29). The oxidation of the RyR results in the dissociation of the RyR-binding protein Calstabin, a member of the diverse FK506 binding protein family (4, 6–11, 28, 30). The dissociation of Calstabin results in a persistent calcium leak through the RyR and reduced muscle contraction (4, 11–20, 28, 30–32). The binding of Calstabin to the oxidized RyR can be re-established via the actions of a 1,4-benzothiazepine derivative (S107) that has been shown to reverse the effects of age on muscle function in mice, resulting in an increased health span (5, 21–25, 28, 33). This is similar to what has been observed with administration of the SS-31 peptide to aged mice, which has been shown to improve muscle function as a result of improved mitochondrial function in skeletal muscle, supporting the idea that increased oxidative stress

* This work was supported by National Institutes of Health RO1 Award NS062811 (to B. A. E.) and Biology of Aging Training Grant T32 AG021890 (to R. E. M.). The authors declare that they have no conflicts of interest with the contents of this article. The content is solely the responsibility of the authors and does not necessarily represent the official views of the National Institutes of Health.

[1] To whom correspondence should be addressed: Dept. of Integrative and Cellular Physiology, University of Texas Health Sciences Center at San Antonio, 7703 Floyd Curl Dr., San Antonio, TX 78229. Tel.: 210-567-4383; Fax: 210-567-4410; E-mail: eatonb@uthscsa.edu.

[2] The abbreviations used are: RyR, ryanodine receptor; PER, proboscis extension reflex; CM9, cibarial muscle 9; NMJ, neuromuscular junction; EJP, endplate junctional potential; mEJP, miniature endplate junctional potential; 4-HNE, 4-hydroxynonenal; DNPH, 2,4-dinitrophenylhydrazine; NMR, naked mole rat; ANOVA, analysis of variance.

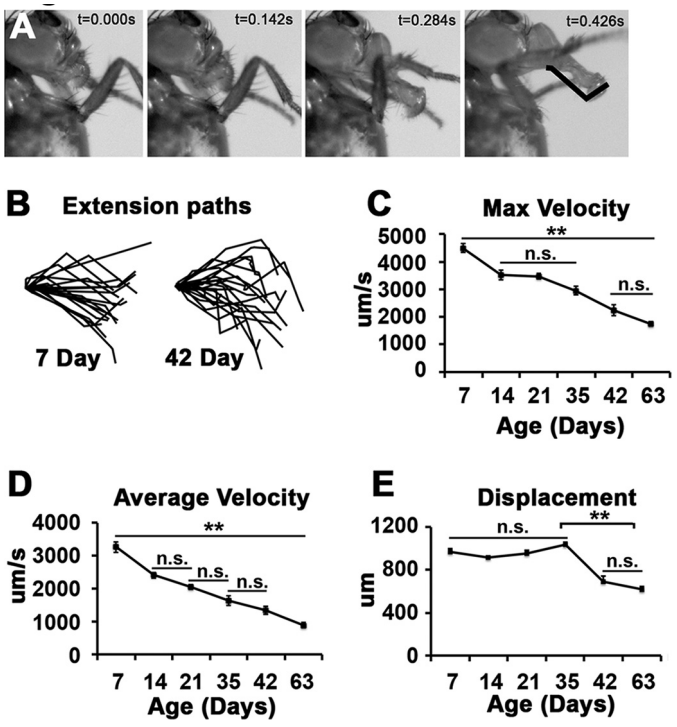

FIGURE 1. **Age-dependent decline in motor function.** *A*, images from time lapse video of PER from a 7-day-old animal are subjected to bristle tracking. Bristle path indicated in last frame and event time indicated at *top right*. *B*, representative bristle paths from 7- and 42-day-old wild type flies (18 paths from 9 flies/age). *C–E*, graphs represent the average value for maximum (*C*), average velocity (*D*), and linear displacement (*E*) determined from the bristle path analysis of PERs from 7–63-day-old wild type flies (14–28 events from 9–14 flies). *Error bars* indicate S.E. All significant differences were determined using ANOVA. **, $p < 0.01$.

in skeletal muscle is an important cause of compromised muscle function during aging (34).

Results

S107 Restores Muscle Function during Aging in Drosophila—To investigate the effects of age on muscle function in *Drosophila*, we utilized a simple motor reflex in flies known as the proboscis extension reflex (PER) (35). The activation of the muscles controlling proboscis is motor neuron-dependent and utilizes a classic excitation:contraction coupling mechanism similar to mammalian skeletal muscles. Bristles on the tip of the proboscis were tracked during an extension event using high speed video microscopy and particle tracking software (Fig. 1*A*). Extension paths were generated from acquired PER videos, allowing for quantification of maximum velocity, average velocity, and the linear displacement of the tip of the proboscis (Fig. 1*B*). We observed a continuous and significant reduction in both maximum (Fig. 1*C*) and average velocity (Fig. 1*D*) of the proboscis extension. Although velocities decline continuously throughout the life span, we observe an abrupt change in the linear displacement of the proboscis between 35 and 42 days of age (Fig. 1*E*). Because this change in displacement correlates strongly with the age-dependent potentiation of neurotransmitter release we previously demonstrated at the cibarial muscle 9 neuromuscular junction (CM9 NMJ) (36), we believe that this change in displacement is related to this change in motor neuron output and not muscle physiology.

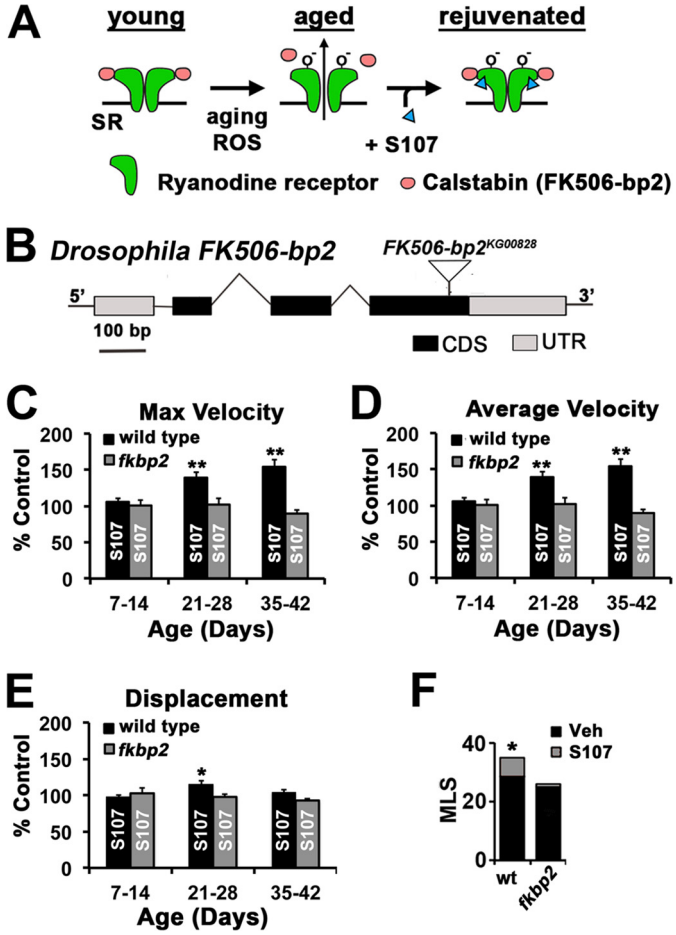

FIGURE 2. **S107 improves proboscis extension and survival.** *A*, a model of age-dependent oxidation of RyR and the restorative effect of S107. *B*, a schematic of a *Drosophila FK506-BP2*1 gene indicating the coding sequences (*CDS*), untranslated regions (*UTR*), and the location of the P-element (*FK506-BP2*^{KG00828}). *C–E*, graphs represent the percentage of increase *versus* control (vehicle only) in flies fed S107 for indicated 1 week period in maximum (*C*), average velocity (*D*), and displacement (*E*) from wild type (*black bars*) and *FK506-BP2* (*fkbp2*) mutant flies (*gray bars*). Average values were normalized to vehicle control values for each condition ($n = 14–19$ events from 7–10 flies). Significance was determined by Student's *t* test between S107 *versus* vehicle for each condition. *, $p < 0.05$; **, $p < 0.01$. *Error bars* indicate S.E. *F*, median life span was calculated for wild type (*wt*) and *FK506-BP2* (*fkbp2*) between 35 and 90 days. Significance was determined by log rank test. *, $p < 10^{-6}$. *MLS*, median life span; *Veh*, vehicle.

The age-dependent decline in skeletal muscle function in mammals has been attributed to the oxidation-dependent dissociation of the Calstabin accessory protein from the RyR (28). The drug S107 has been shown to reverse the effects of age on muscle function presumably by re-establishing the binding of Calstabin (also known as FKBP12.1) to the oxidized RyR, thereby providing a pharmacological method for investigating the role of this mechanism in the decline in proboscis extension velocities (Fig. 2*A*). Because the effects of S107 are believed to be due to the stabilization of the binding of Calstabin to the RyR, we utilized a mutation in the putative *Drosophila calstabin* homologue *FK506-BP2* to control for the effects of S107 in these experiments (28, 33). The product of the *FK506-BP2* locus shares over 75% amino acid identity with both murine and human Calstabin proteins. To investigate whether this gene product is required for the effects of S107, we utilized a fly line carrying a P-element insertion ($P^{FK506\text{-}BP2\ KG00828}$) that dis-

TABLE 1

Analysis of the effects of S107 on proboscis extension

The *FK506-bp2* mutation utilizes the lab w^{1118} stock (wild type) as the genetic background. Age is presented as the treatment window in days post-eclosion with analysis occurring on final treatment day. All of the values represent averages with S.E. presented in parentheses. *N* represents the number of animals analyzed (16–28 events/animal). The values for the treatment window 35–42 days were collected in separate experiments from other treatment groups. veh, vehicle.

Genotype	Age	Condition	Maximum velocity	Average velocity	*N*
			μm/s	*μm/s*	
w^{1118}	7–14	+ veh −	5516 (269)	3666 (215)	12
w^{1118}	7–14	+ S107	5388 (221)	3863 (213)	11
w^{1118}	21–28	+ veh	3929 (267)	2582 (209)	8
w^{1118}	21–28	+ S107	5398 (200)[a]	3594 (184)[a]	10
w^{1118}	35–42	+ veh	2936 (205)	1528 (101)	10
w^{1118}	35–42	+ S107	3992 (168)[a]	2349 (162)[a]	9
FK506-bp2	7–14	+ veh −	4321 (146)	2810 (117)	14
FK506-bp2	7–14	+ S107	4098 (239)	2845 (201)	8
FK506-bp2	21–28	+ veh	3816 (233)	2693 (181)	8
FK506-bp2	21–28	+ S107	3989 (244)	2740 (236)	11
FK506-bp2	35–42	+ veh	3170 (231)	1928 (125)	13
FK506-bp2	35–42	+ S107	3348 (138)	1739 (80)	11

[a] Indicates values that are significantly different than corresponding vehicle controls determined by Student's *t* test.

rupts the *Drosophila FK506-BP2* gene (Fig. 2*B*). Because this allele will be used to control for off target effects of S107, this P-element was backcrossed 10 generations to our wild type strain (w^{1118}) and assayed as a homozygotic *FK506-BP2* mutant to minimize differences in genetic backgrounds. Virgin wild type and *FK506-BP2* flies of various ages were fed food supplemented with S107 or vehicle for 7 days prior to assaying motor function using PER. S107 data are presented as normalized to vehicle control for each treatment group to help illustrate the age-dependent effects of S107 on motor function. All average values from these analyses are presented in Table 1. We find that treatment of wild type flies with S107 significantly improved maximum (Fig. 2*C*, *black bars*) and average velocity (Fig. 2*D*, *black bars*) at 28 and 42 days of age but not at 14 days of age. We also observe that the magnitude of the effects of S107 on extension velocity in wild type increases with age (Fig. 2, *C* and *D*, *black bars*). Both of these effects of S107 are absent in *FK506-BP2* mutant flies (Fig. 2, *C* and *D*, *gray bars*). There was also no effect of S107 on displacement, supporting the idea that this phenotype is not a result of declining muscle function (Fig. 2*E*). These data are consistent with an evolutionarily conserved effect of S107 during age-dependent motor dysfunction.

We predicted that declining motor functions would be a key contributor to mortality in our fly colonies. To test this possibility, we determined the effects of S107 on survival. Life span data were collected from wild type and *FK506-BP2* flies raised on normal food to 35 days of age when flies were split into two groups with one group receiving food supplemented with S107 and the other group receiving food treated with vehicle (control). Despite being put on S107 at 35 days of age, the mean life span of wild type flies after treatment was significantly different compared with the flies fed vehicle only resulting in an increase in the mean survival post-drug of 19.6% (Fig. 2*F*, *gray bars*). It should be noted that these life span analyses were terminated after all animals receiving the vehicle supplemented food died to conserve drug; thus the effects of drugs on mean survival are underestimated. At the termination of the experiment, 12% of the initial cohort of wild type flies receiving the S107 supplemented food remained alive. In parallel experiments, S107 had no effect on survival when fed to *FK506-BP2* mutant flies, and all mutant flies died in these cohorts (Fig. 2*F*). We also observe that *FK506-BP2* mutant control flies have a reduced mean life span (Fig. 2*F*, *black bars*). Collectively, these data demonstrate that S107 can extend health span and life span in an *FK506-BP2*-dependent fashion.

We wondered whether the effects of S107 on PER are due to increased neurotransmission at the NMJ. To investigate this possibility, we analyzed synaptic transmission at the CM9 NMJ from 14- and 42-day-old wild type animals treated with S107 for 7 days. This NMJ is located on the CM9 muscle group of the proximal proboscis and is known to participate in proboscis extension (35, 37). We observe no significant difference in the amplitude or shape of miniature end plate junctional potentials (mEJPs) between animals treated with vehicle and S107, demonstrating no change in the sensitivity of muscle to the excitable effects of neurotransmitter (Fig. 3, *B* and *F*). We also did not observe differences in the resting membrane potentials or input resistance (Table 2). These data reveal that S107 has no effect on the electrical properties of the muscle. We did observe that average amplitudes of evoked EJPs are significantly reduced in 42-day-old animals treated with S107 (Fig. 3, *E* and *G*) compared with 14-day-old animals (Fig. 3, *A* and *C*). Analysis of quantal content (the number of vesicles released per EJP) revealed that this specific reduction in EJP amplitudes at 42-day-old NMJs in animals fed S107 compared with 14-day-old NMJs was the result of a significant reduction in neurotransmitter release (Fig. 3, *D* and *H*). These interesting results suggest that the age-dependent potentiation in neurotransmission could be compensatory for declining motor function (36). Importantly, these data demonstrate that the improvement of motor function in 42-day-old flies by S107 is not the result of increased neurotransmission.

The Effects of Age and Oxidative Stress on Muscle Function Require the Drosophila FK506-BP2 Gene—Using our PER assay, we observed that *FK506-BP2* mutants have reduced values for maximum and average velocities compared with wild type flies analyzed in parallel between 7 and 35 days of age, demonstrating that FK506-BP2 is required for normal muscle function during this early period in the life of the fly (Fig. 4, *A* and *B*). Furthermore, the magnitude of the reduction in extension velocities that we observe in our *FK506-BP2* mutants compared with controls at 7 days (~25%) is quantitatively similar to what was reported for the change in contractile force in muscle fibers isolated from young Calstabin-KO mice compared with young wild type mice, supporting the evolutionarily conserved nature of FK506-BP2 function (28). These data are consistent with channel studies demonstrating a modulatory and not obligatory role for Calstabin/FKBP12.6 for RyR gating during muscle contraction (30, 38). Although initial velocity is reduced in FK506-BP2 mutants, we observe that *FK506-BP2* mutants actually have significantly increased extension velocities at 42 days of age compared with wild type flies (Fig. 4, *A* and *B*). Between 42 and 63 days of age, the extension velocities in *FK506-BP2* mutants declined precipitously, resulting in flies with visibly impaired motor function. To investigate whether these observations extend to other motor behaviors, we com-

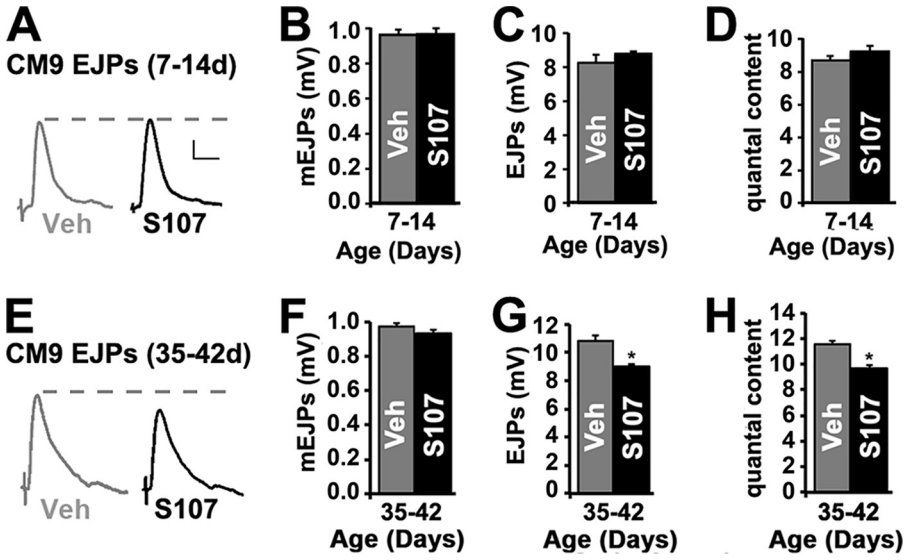

FIGURE 3. **Effect of S107 on neurotransmission at the CM9 neuromuscular junction.** *A*, CM9 evoked EJP traces from 14-day-old wild type flies fed vehicle (*gray trace*) or S107 (*black trace*) from 7 to 14 days of age. *B–D*, graphs represent average values for mEJPs (*B*), evoked EJPs (*C*), and quantal content (*D*) in recordings from the CM9 NMJs on day 14 in flies from the indicated 7–14-day treatment group. *E*, CM9 EJP traces from 42-day-old wild type flies fed vehicle (*gray trace*) or S107 (*black trace*) from 35 to 42 days of age. *F–H*, graphs represent average values for mEJPs (*F*), evoked EJPs (*G*), and quantal content (*H*) in recordings from the CM9 NMJs on day 42 in flies from the indicated 35–42-day treatment group. *Error bars* indicate S.E. Significance was determined by Student's *t* test. *, $p < 0.05$. *Veh*, vehicle.

TABLE 2
Morphological and electrophysiological analysis of *FK506-bp2* mutants

Genotype	CM9 muscle fibers[a]	Myonuclei/μm[b]	mEPSP amplitude	mEPSP half-width	EPSP amplitude	RM	I_R[c]
			mV		*mV*	*mV*	*MΩ*
W^{1118}	15 (0)	0.1165 (0.0083)	0.99 (0.01)	8.17 (0.76)	9.07 (0.37)	−38.17 (2.40)	9.25 (0.75)
FK506-bp2	15 (0)	0.1390[a] (0.0074)	0.99 (0.05)	7.31 (0.79)	9.37 (0.36)	−39.92 (1.72)	9.75 (0.80)

The *FK506-bp2* mutation utilizes the lab w^{1118} stock (wild type) as the genetic background. All values represent averages with S.E. presented in parentheses.
[a] The values for fibers obtained from CM9 muscle groups from 5 animals/genotype. The values for myonuclei density obtained from 20 fibers/genotype.
[b] Indicates values that are significantly different than wild type determined by Student's *t* test.
[c] The values represent the average from 8 animals/genotype.

pared the wall climbing of wild type flies and *FK506-BP2* mutants and found that wild type flies outperformed *FK506-BP2* mutant flies at 30 days of age but that *FK506-BP2* mutants outperformed wild type at 45 days of age (Fig. 4*C*). To control for the effects of *FK506-BP2* mutations on muscle development or excitability, we examined the morphology of CM9 muscle fibers in 7-day-old *FK506-BP2* mutants and found no significant difference in the number of muscle fibers or myonuclei morphology compared with wild type (Fig. 4*D* and Table 2). Additionally, analysis of *FK506-BP2* mutant electrophysiology revealed no significant difference in muscle excitability (Table 2). These data demonstrate that the effect of *FK506-BP2* mutants on muscle function in young animals is not due to changes in muscle excitability or gross muscle morphology.

To determine whether the decrease in muscle function observed in young *FK506-BP2* mutants is due to the loss of *FK506-BP2* function specifically in the muscle, we performed transgenic rescue experiments by expressing a *UAS-FK506-BP2* transgene in the muscles of *FK506-BP2* mutants using a muscle Gal4 driver (*MHC-Gal4*). Muscle expression of wild type FK506-BP2 in *FK506-BP2* mutants rescued the defects in maximum and average velocities observed in 7-day-old flies (Fig. 4, *E* and *F*, *red squares*). Furthermore, the expression of FK506-BP2 within the muscle of *FK506-BP2* mutant restores muscle function, including the progressive declines in motor function observed between 7 and 35 days of age in wild type flies (Fig. 4, *E* and *F*, *red squares*; see Fig. 4, *A* and *B* for wild type comparison). Neuronal expression of FK506-BP2 in *FK506-BP2* mutants using the panneuronal *C155-Gal4* driver failed to rescue motor function (data not shown).

Based on the existing data from the mouse, the oxidation of the RyR receptor results in the dissociation of the Calstabin, leading to compromised muscle function in aged animals (28). To investigate this hypothesis, we induced oxidative stress with paraquat in young flies and assayed the effects on motor function. Both wild type and *FK506-BP2* mutant flies were raised on normal aging food until 7 days of age and assayed for motor function. Remaining flies were split to three different food conditions: 1) vehicle, 2) a sublethal concentration of paraquat, or 3) paraquat + S107 (Fig. 5*A*). The flies were maintained on these conditions for 7 days and then re-evaluated for motor function. We found that treating the young wild type flies with paraquat for 7 days resulted in a significant decrease in maximum (Fig. 5*B*, *black squares*) and average (Fig. 5*C*, *black squares*) velocities compared with vehicle alone (Fig. 5*B* and *C*, *gray diamonds*). Importantly, adding S107 to paraquat food completely reversed the effects of paraquat and restored both maximum and average velocity to control values (Fig. 5, *B* and *C*, *red triangles*). To verify that the paraquat treatment increased oxidative stress, flies subjected to these treatment con-

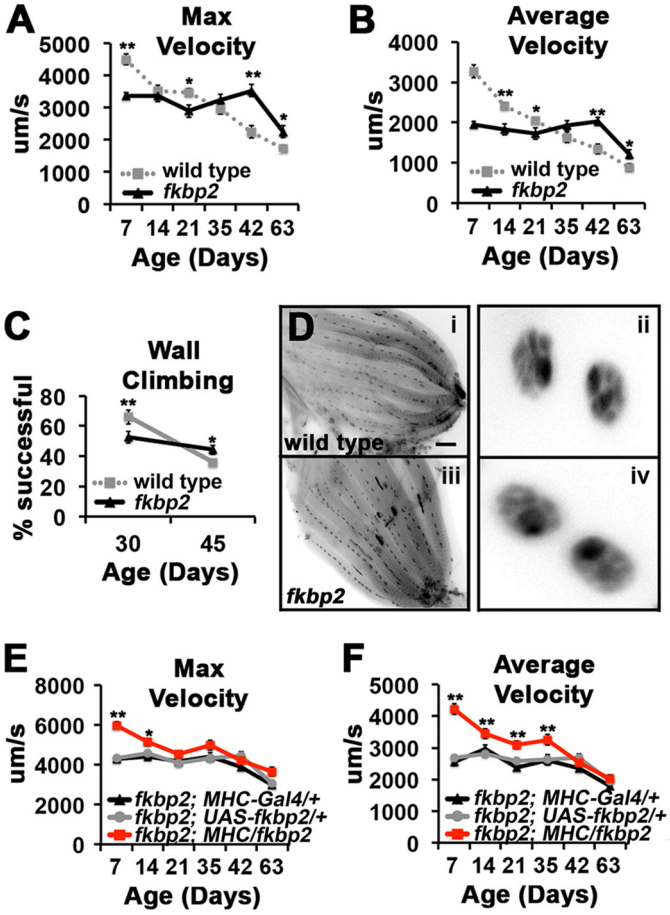

FIGURE 4. **Effects of *FK506-BP2* mutants on motor function during aging.** *A* and *B*, graphs present average value for maximum (*A*) and average velocity (*B*) for wild type (*gray dotted line*, from Fig. 1, *C* and *D*) and *FK506-BP2* (*fkbp2*) flies (*black line*) from 7 to 63 days of age ($n = 16–28$ events from 8–16 flies). *Error bars* indicate S.E. Significance was determined by Student's *t* test of *FK506-BP2 versus* wild type for each time point. *, $p < 0.05$; **, $p < 0.01$. Note that these data were collected in parallel. *C*, graphs represent the percentage of total number of flies that reach the threshold of 8 cm in 10 s for wild type (*gray squares*) and *FK506-BP2* (*fkbp2*) flies (*black triangles*) ($n = 120–200$ flies/genotype). *Error bars* indicate S.E. Significance was determined by Student's *t* test of *FK506-BP2 versus* wild type for each time point. *, $p < 0.05$; **, $p < 0.01$. *D*, inverted images of CM9 muscle group from 7-day-old wild type (*panel i*) and *FK506-BP2* (*fkbp2*) flies (*panel iii*) stained with antibodies to Discs-large and DAPI. Enlarged are representative myonuclei from wild type (*panel ii*) and *FK506-BP2* (*fkbp2*) (*panel iv*) fibers. *E* and *F*, graphs represent the average values for maximum (*E*) and average velocity (*F*) determined from 7 to 63 days of age in *FK506-BP2* (*fkbp2*) mutant flies containing the *MHC-Gal4* driver (*fkbp2*; *MHC-Gal4/+*; *black triangles*), the *UAS-FK506-BP2* transgene (*fkbp2*; *UAS-fkbp2*; *gray circles*), and *FK506-BP2* mutant flies expressing the FK506-BP2 solely in the muscle (*fkbp2*; *MHC/fkbp2*; *red squares*) ($n = 30–42$ events from 13–21 flies). *Error bars* indicate S.E. Significance was determined using ANOVA. *, $p < 0.05$; **, $p < 0.01$.

ditions were subjected to immunoblot analysis of the 4-hydroxynonenal (4-HNE) product of lipid oxidation, which has been used previously to monitor oxidative stress in *Drosophila* (Fig. 5, *D–F*) (39, 40). Not only do we observe a significant increase in 4-HNE adducts under our paraquat treatment conditions, the inclusion of S107 did not blunt the effect of paraquat on the generation of oxidative stress (Fig. 5, *D–F*).

Unlike the wild type flies, feeding *FK506-BP2* mutants paraquat for 7 days did not result in a significant decrease in either maximum (Fig. 5*G*, *black squares*) or average (Fig. 5*H*, *black squares*) velocities. Furthermore, adding S107 to food supplemented with paraquat did not have any effect on either maximum or average velocities in *FK506-BP2* mutants (Fig. 5, *G* and *H*, *red triangles*). Analysis of 4-HNE adducts demonstrates that feeding paraquat (Fig. 5, *I–K*, *black bars*) and paraquat + S107 (Fig. 5, *I–K*, *red bars*) to *FK506-BP2* mutants significantly increased the formation of 4-HNE adducts (Fig. 5, *I–K*), similar to what is observed in wild type (Fig. 5, *D–F*). These data demonstrate that paraquat has no effect on motor function in *FK506-BP2* mutants.

We wanted to confirm that the RyR is oxidized under our experimental conditions. The chromosome deficiency, *Df BSC269*, lacks the region containing the *RyR* gene and was used as a null allele in these studies. We found reduced levels of RyR protein in the heterozygotic *DfBSC269*/+ mutant (RyR^{Df}/+) compared with wild type controls supporting the specificity of the *Drosophila* RyR antibody (Fig. 6, *A* and *B*). To determine whether the RyR gets oxidized as flies age, we subjected young (7 and 14 days old) and old (55 days old) flies to both fractionation and immunoprecipitation purification of RyRs followed by immunoblot analysis of 2,4-dinitrophenylhydrazine (DNPH) derivation of protein carbonyls and RyR receptor cysteine nitrosylation. This approach has been previously used to assay the level of RyR protein oxidation in mouse cardiac muscle (28). We observed that the RyRs from aged flies (55 days old) exhibit increased oxidation compared with young animals (7 and 14 days old) (Fig. 6, *C*, *D*, *E*, *J*, and *K*). In addition, the effect of age on RyR oxidation was phenocopied in our young flies being fed paraquat from 7 to 14 days of age (Fig. 6, *F–K*). These analyses demonstrate that the *Drosophila* RyR is oxidized during aging and in response to paraquat-induced oxidative stress.

To verify that the effects of paraquat on motor function were due to FK506-BP2 function in muscle, 7-day-old *FK506-BP2* mutant flies expressing wild type FK506-BP2 only in the muscle were treated with paraquat for 7 days and assayed for PER. The expression of FK506-BP2 in *FK506-BP2* mutant muscle completely restored the sensitivity of motor function to paraquat compared with controls (Fig. 7, *A* and *B*, *red triangles*). It should be noted that in these experiments, we observed that the viability of the *MHC-Gal4*/+ control stock was compromised in the presence of paraquat, and the animals did not survive the handling during the PER analysis. Taken together, these data support the model that the effects of paraquat on motor function require FK506-BP2 function in the muscle.

We also observe that muscle overexpression of FK506-BP2 in 7-day-old flies provides protection against the effects of paraquat on proboscis extension, similar to what we observe with S107 (Fig. 7, *C* and *D*). This suggests that bound FK506-BP2 can protect the RyR from oxidation. In addition, the overexpression of FK506-BP2 also provides some protection against the declines in motor function observed during age (Fig. 7, *E* and *F*). Interestingly, the magnitude of the effects of FK506-BP2 overexpression is much less in 42-day-old animals (13–18% increase *versus* controls) compared with what we observe for S107 (51–55% *versus* controls; Fig. 2). These suggest that S107 is more potent in rejuvenating motor function in older flies than overexpression of FK506-BP2. One possibility is that S107 is able to overcome the effects of oxidation on the function of the RyR,

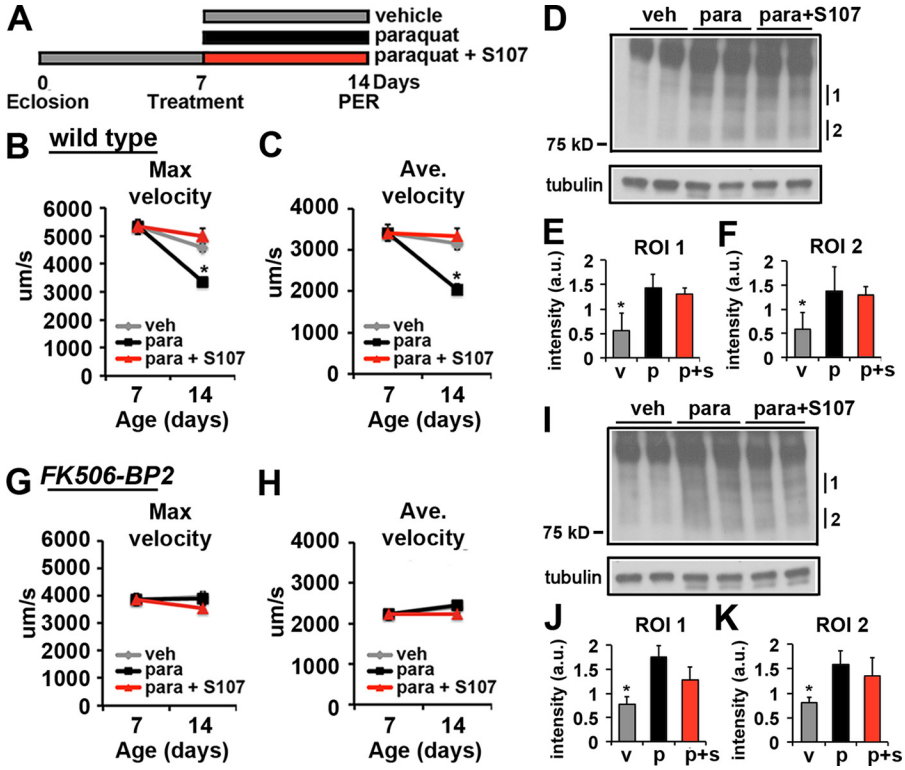

FIGURE 5. **Effects of paraquat on proboscis extension in wild type and *FK506-BP2* mutant flies.** *A*, schematic depiction of the experimental design. *B* and *C*, graphs represent average values for maximum (*B*) and average velocity (*C*) on days 7 and 14 of wild type flies treated with vehicle (*veh*, *gray diamonds*), paraquat (*black squares*), and paraquat + S107 (*red triangles*) from 7 to 14 days of age ($n = 23$–32 events from 12–16 flies). *Error bars* indicate S.E. Significance was determined using ANOVA. *, $p < 0.05$; **, $p < 0.01$. *D*, immunoblot of 4-HNE-modified proteins from 14-day-old whole wild type fly extracts treated with vehicle, paraquat, and paraquat + S107 from 7 to 14 days of age. Tubulin is shown as a loading control. *E* and *F*, graphs represent average value for intensity of regions of interest (*ROI*) indicated in *D* normalized to tubulin. *v*, vehicle (*gray bars*); *p*, paraquat (*black bars*), *p + s*, paraquat + S107 (*red bars*) ($n = 4$). *Error bars* indicate S.D. Significance was determined using ANOVA. *, $p < 0.05$. *G* and *H*, graphs represent average values for maximum (*G*) and average velocity (*H*) on days 7 and 14 from *FK506-BP2* flies treated with vehicle (*gray diamonds*), paraquat (*black squares*), and paraquat + S107 (*red triangles*) from 7 to 14 days of age ($n = 25$–32 events from 14–16 flies). *Error bars* indicate S.E. Significance was determined using ANOVA. *, $p < 0.05$; **, $p < 0.01$. *I*, immunoblot of 4-HNE-modified proteins from 14-day-old whole *FK506-BP2* fly extracts treated with vehicle, paraquat, and paraquat + S107 from 7 to 14 days of age. Tubulin is shown as a loading control. *J* and *K*, graphs represent average value for intensity of regions of interest indicated in *I* normalized to tubulin. *v*, vehicle (*gray bars*); *p*, paraquat (*black bars*); *p + s*, paraquat + S107 (*red bars*) ($n = 4$). *Error bars* indicate S.D. Significance was determined using ANOVA. *, $p < 0.05$.

whereas FK506-BP2 overexpression only modulates the function of the unoxidized RyR (Fig. 7*G*) (33).

Discussion

Loss of FK506-BP2 Function in Muscle Contributes to Health Span in Drosophila—In this study, we have used the *Drosophila* PER as a proxy for muscle function to investigate the role of FK506-BP2 and oxidative stress in age-related declines in motor function. Our data demonstrate that the declines in extension velocities observed during young to mid-life require FK506-BP2 function in the muscle. This model is strongly supported by our genetic rescue data demonstrating that muscle expression of FK506-BP2 in *FK506-BP2* mutants is able to rescue the declines in extension velocities observed during the early stages of life. Furthermore, we observe that feeding wild type flies S107, a drug that restores FK506-BP2 binding to oxidized RyRs, completely reverses the decline in motor function. Importantly, this effect of S107 on muscle function is absent in the *FK506-BP2* mutant. In addition, the effect of S107 is dependent upon the age of the animal because feeding young flies S107 has no effect on motor function. Moreover, we found that supplementing our lab diet with S107 is sufficient to extend life span in aged wild type flies but not *FK506-BP2* mutants, demonstrating that the effects of S107 on health span and life span require FK506-BP2 function. Because mammalian models have also shown that loss of FK506-BP2 binding caused by RyR oxidation results in a decline in health span (28), these data support the idea that the oxidation of the RyR and the subsequent loss of Calstabin binding is an evolutionarily conserved event that contributes to declines in health span. Although we did not directly demonstrate the dissociation of FK506-BP2 from the RyR in our system, we did provide evidence of the oxidation of the RyR in response to both age and paraquat supporting this hypothesis.

The age-dependent loss of motor function that we observe in young animals appears to be the result of increasing oxidative stress because it is phenocopied by feeding young animals paraquat, a compound that poisons the electron transport systems in mitochondria resulting in enhanced oxidative stress (41). Further, the effects of this potent oxidative stressor on muscle function are completely reversed by S107. The effects of paraquat on muscle function are dependent upon FK506-BP2 because *FK506-BP2* mutant flies lack the effects of paraquat on muscle function and muscle-specific rescue of *FK506-BP2* mutants restores the sensitivity of muscle function to paraquat. This is similar to what we observe with the requirement for

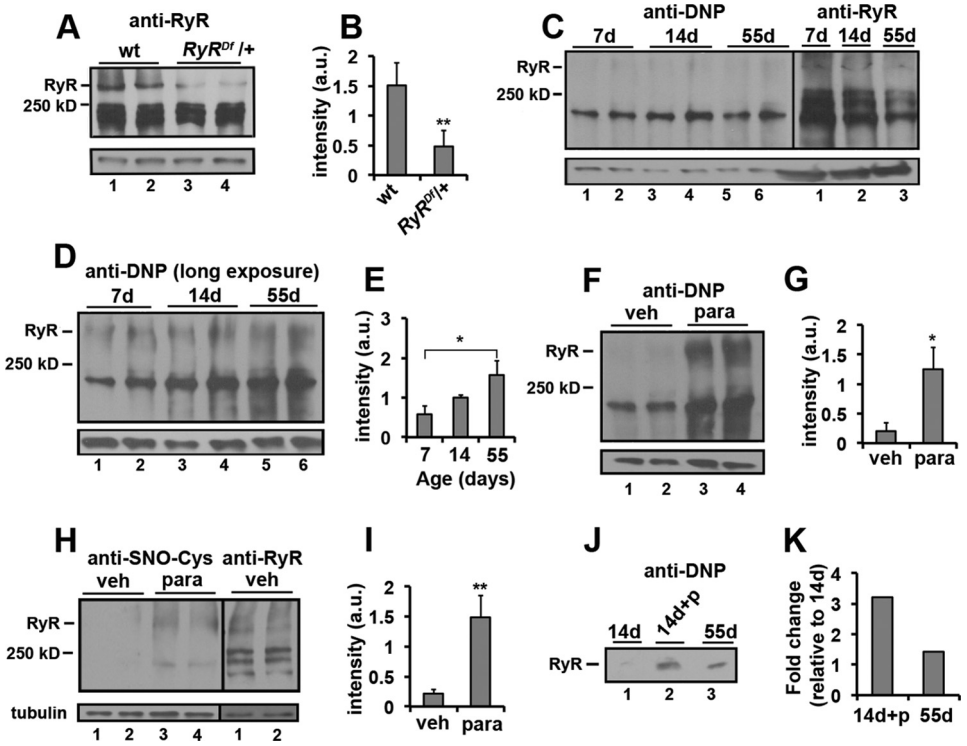

FIGURE 6. **Effects of age and paraquat on oxidation of *Drosophila* ryanodine receptors.** *A*, immunoblot analysis of wild type (*wt*; *lanes 1* and *2*) and RyR/+ (RyR^{Df}; *lanes 3* and *4*) fly extracts probed with anti-dRyr antibody. *B*, bar graph represents quantification of the immunoblot in A ($n = 4$). *C*, *left panel*, immunoblot analysis of DNPH-treated proteins from 7- (*lanes 1* and *2*), 14- (*lanes 3* and *4*), and 55-day-old (*lanes 5* and *6*) whole wild type fly extracts probed with anti-DNP antibody. *Right panel*, immunoblot analysis of 7- (*lane 1*), 14- (*lane 2*), and 55-day-old (*lane 3*) whole wild type fly extracts probed with anti-RyR antibody from the same blot. *D*, long exposure of DNP immunoblot shown in *C*. *E*, bar graph represents quantification of the anti-DNP immunoblot in *D* ($n = 4$). *F*, immunoblot analysis of DNPH-treated proteins from 14-day-old whole wild type fly extracts treated with vehicle (*veh*; *lanes 1* and *2*) and paraquat (*para*; *lanes 3* and *4*) from 7 to 14 days of age. *G*, bar graph represents quantification of the immunoblots in *F* ($n = 2$). *H*, *left panel*, immunoblot analysis of 14-day-old whole wild type fly extracts treated with vehicle (*veh*; *lane 1*,2) and paraquat (*para*; *lanes 3* and *4*) from 7 to 14 days of age probed with anti-SNO-Cys antibody. *Right panel*, immunoblot analysis of 14-day-old whole wild type fly extracts treated with vehicle probed with anti-RyR antibody from the same blot. *I*, bar graph represent quantification of the immunoblot in H ($n = 4$). *J*, immunoblot analysis of DNPH-treated proteins from 14-day-old wild type fly extracts treated with vehicle (*lane 1*) and paraquat (+*p*; *lane 2*) and 55-day-old (*lane 3*) wild type fly extracts immunoprecipitated with anti-RyR antibody. *K*, bar graph represents quantification of the immunoblot in *J* ($n = 1$). Tubulin is shown as a loading control in *A*, *C*, *D*, *F*, and *H*. Bar graphs (*B*, *E*, *G*, and *I*) represent average values for intensity of the RyR band normalized to tubulin. *Error bars* indicate S.D. Significance was determined using a Student's *t* test (*B*, *G*, and *I*) or ANOVA (*E*). *, $p < 0.05$; **, $p < 0.01$. *d*, day.

FK506-BP2 during the effects of aging on muscle function. Combined with our biochemical data, these results support the hypothesis that the effects of age and paraquat on motor function require *FK506-BP2* expression in the muscle. These results are consistent with recent work from mice showing that mitochondria engineered to overexpress catalase protects against RyR oxidation, subsequent FK506-BP2 dissociation, and muscle weakness (42).

These data support the oxidative stress theory of aging in which reactive oxygen species generated during normal cellular metabolism cause oxidant damage to proteins and lipids, resulting in decreasing cellular function. Our data also highlight a singular cellular component that is sufficient to alter both health span and life span in response to oxidative stress. In our experiments, it is unclear exactly how motor function contributes to mortality, and it is possible that the effects of S107 on life span are due to restoration of FK506-BP2 function in a non-muscle tissue. Perhaps enhanced muscle function could increase survival because of a general requirement of movement for optimal fitness including proximal requirements such as avoiding accidents (getting stuck in food), grooming, and feeding. Although it is likely that the contribution of declining motor function to health span and life span will be different for different species, the effects of FK506-BP2 dysfunction on human skeletal and cardiac muscle function is clear (43–45). Therefore it is likely that RyR oxidation represents an important age-dependent morbidity in both vertebrates and invertebrates and represents an exciting target for the extension of human health span and life span.

Aging in FK506-BP2 Mutants—We find that extension velocity is significantly higher in 42-day-old *FK506-BP2* mutant flies than age-matched controls, despite the fact that young *FK506-BP2* mutants have reduced initial extension velocities. This effect of *FK506-BP2* mutants on motor function is also reflected in our wall climbing assays that find that the 45-day-old *FK506-BP2* mutants outperform age-matched controls. We believe that a key difference between a 45-day-old wild type and a 45-day-old *FK506-BP2* mutant is the presence of FK506-BP2 in the cytosol of wild type muscles that has dissociated from the RyR in response to oxidation. Perhaps this pool of liberated FK506-BP2 participates in a compensatory signaling system that changes RyR function during high intensity contraction conditions to protect the muscle from the effects of increased calcium discharges from the SR. In *FK506-BP2* mutants, this signal is absent, and calcium discharge remains increased into later life resulting in a stress-induced muscle failure that man-

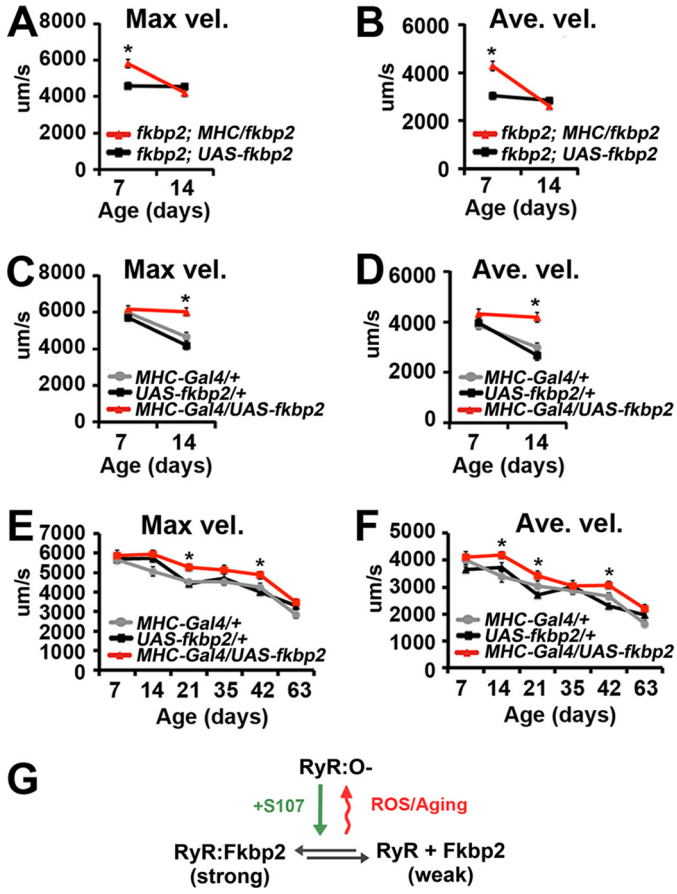

FIGURE 7. **FK506-BP2 in muscle is responsible for paraquat resistance.** *A* and *B*, graphs represent the average value for maximum (*Max vel.*, *A*) and average velocity (*Ave. vel.*, *B*) on days 7 and 14 for *FK506-BP2* (*fkbp2*); *UAS-FK506-BP2* (*fkbp2*) control stock (*black squares*) and *FK506-BP2* (*fkbp2*) mutants expressing FK506-BP2 only in the muscles (*fkbp2*; *MHC/fkbp2*; *red triangles*) treated with paraquat from 7 to 14 days of age ($n = 16–34$ events from 8–17 animals). *C* and *D*, graphs represent average values for maximum (*C*) and average velocity (*D*) on days 7 and 14 for *MHC-Gal4* driver (*gray circles*), *UAS-FK506-BP2* (*fkbp2*) (*black squares*), and *FK506-BP2* (*fkbp2*) muscle overexpression (*red triangles*) flies treated with paraquat from 7 to 14 days of age. *Error bars* indicate S.E. Significance was determined using a Student's *t* test (*A* and *B*) or one-way ANOVA (*C* and *D*). *, $p < 0.05$. *E* and *F*, graphs represent average values for maximum (*E*) and average velocity (*F*) determined from 7 to 63 days of age for *MHC-Gal4* (*gray circles*), *UAS-FK506-BP2* (*fkbp2*) (*black squares*), and *FK506-BP2* (*fkbp2*) muscle overexpression (*red triangles*) flies ($n = 17–41$ events from 15–22 flies). *Error bars* indicate S.E. Significance was determined using ANOVA. *, $p < 0.05$; **, $p < 0.01$. *G*, the oxidation of the RyR limits the effectiveness of FK506-BP2 (Fkbp2) overexpression on motor function with increasing age. S107 promotes FK506-BP2 (Fkbp2) binding to the oxidized RyR overcoming this effect of increasing age on muscle function.

ifests in our system as the precipitous decline in extension velocities that we observe from 42 to 62 days of age in *FK506-BP2* mutants. This possibility is supported by the observations that increased calcium discharge resulting from exercise induced oxidation is able to activate the calcium-dependent calpain protease (29) and the finding that mice lacking Calstabin/FKBP12.6 are highly susceptible to exercise-induced sudden cardiac arythmia (46).

The prolonged maintenance of motor function with age in *FK506-BP2* mutants is reminiscent of recent studies showing that the extraordinarily long-lived rodent, the naked mole rat (NMR) maintains cardiac function, as measured by fractional shortening, well into its third decade of life, much longer than the equivalently sized mouse (47). However, all of the markers of cardiac function are indicative of a very low basal systolic function in NMRs, similar to the reduced motor function observed in *FK506-BP2* mutants (47). It is interesting to note that NMRs are known to have much higher levels of protein oxidation compared with other mammals (22). Perhaps this phenocopy with our *FK506-BP2* mutants indicates that FK506-BP2 is constitutively dissociated from the RyR in the NMR, eliminating this source of age-dependent decline in both cardiac and skeletal muscle function and contributing to the greater tolerance to oxidative stress of the NMR (5). Because NMRs have not been reported to suffer sudden cardiac arrhythmias, it is possible that they have developed a novel compensatory mechanism to deal with the increased cytosolic calcium levels.

Given that *FK506-BP2* mutants have reduced sensitivity to oxidative stress, one might expect that *FK506-BP2* mutants would have increased longevity. Surprisingly, we observe that *FK506-BP2* mutants exhibit a dramatic and abrupt decrease in motor function and reduced life span. One explanation for this observation is that in young animals the liberation of FK506-BP2 from the RyR in response to oxidative stress results in reduced motor function and compromised fitness. Perhaps in aged flies, similar to what we proposed for the effects of soluble FK506-BP2 on motor function, the increasing amount of soluble FK506-BP2 liberated from the RyR also induces cytoprotective processes that are able to extend health span and life span. This possibility is supported by the observations that FKBP12, the FK506-BP2 homologue, participates in signaling systems including TGF-β and mTOR (38, 48). This "hormetic" effect of FK506-BP2 is muted in young animals that have strong binding of FK506-BP2 to the RyR and only contributes to survival late in life. Further, this beneficial effect later in life must provide an advantage to the animal that outweighs the benefits associated with the reduced sensitivity of young *FK506-BP2* mutants to oxidative stress. Understanding how FK506-BP2 function changes with age should provide insight into the cellular effects of oxidative stress and how oxidation contributes to health span and life span.

Experimental Procedures

Fly Stocks—The following genotypes were used: w^{1118} (wild type), *ElaV-Gal4* (C155; Robinow and White, 1988), *MHC-Gal4* (Bloomington Drosophila Stock Center), *P{SUP}FK506-BP2*^{KG00828} (Bloomington Drosophila Stock Center), *Df(2R) Exel6069* (*FK506-BP2*) (Bloomington Drosophila Stock Center), and *Df(2R)BSC269* (*RyR*^{Df}) (Bloomington Drosophila Stock Center). Transgenic *UAS-FK506-BP2* (*fkbp2*) line was generated by microinjection into w^{-1118} (Rainbow Transgenic, Camarillo, CA).

Fly Husbandry and Life Span Analysis—All life span and health span analyses were performed on virgin female flies kept on a 12-h light/dark cycle at 25 °C and 50% humidity on normal lab food (Bloomington Drosophila Stock Center). Flies were flipped to fresh food every 2 days. The *FK506-BP2* allele was backcrossed to the lab w^{1118} for more than 10 generations. For S107 analysis, wild type and *FK506-BP2* flies were kept on normal lab food for 35 days, at which point they were put on food containing 50 μg/ml vehicle (ethanol) (Sigma-Aldrich) or 50

μg/ml S107 (a gift from Andrew R. Marks Lab). The food was prepared daily. Median life span was calculated after treatment. Analysis of the effects of S107 on survival was investigated using a log rank test on mean survival post drug addition and corrected for flies escaped during the analysis ($p < 10^{-6}$).

Proboscis Extension Reflex—Virgin flies of the appropriate age and genotypes were starved and deprived of water for 4–6 h prior to PER analysis as previously described (35). Briefly, digital videos of individual PERs were captured at 9.2 Hz for at least 2 min using Slidebook software (Intelligent Imaging Innovations, Denver, CO). The Slidebook particle tracking feature was used to manually track bristles, and values for average velocity, maximum velocity, and linear displacement were determined for each bristle path. Two paths per animal from 10–20 animals were included in averages. For the effects of S107 and paraquat on muscle function, flies of appropriate age and genotypes were kept on normal food and at appropriate time transferred into vials containing a final concentration of 50 μg/ml S107 (a gift from Andrew R. Marks Lab), 10 mM paraquat (Sigma-Aldrich), or equivalent volumes of vehicle (ethanol).

Molecular Biology—A full-length cDNA for *FK506-BP2* (CG11001) was used as a PCR template for directional TOPO cloning into pENTR (Invitrogen). The Gateway cloning system (Invitrogen, Waltham, MA) and appropriate pUAS-based destination vector was used for microinjection (Drosophila Genomics Resource Center). The presence of the transgene was screened by genomic PCR using primers 5′-CACCATGGGC-GTACAAGTAGTTCCAATTGC-3′ and 5′-CGAGCTGCTC-AAGGTCGAATAG-3′. The location of the *P{SUP}FK506-BP2^{KG00828}* P-element was verified by genomic PCR for disruptions of CG11001 (*FK506-BP2*) using primers 5′-CCAA-CTCCACCCTCACCTTCG-3′ and 5′-CGACGAGCCG-AAGAACATCAT-3′.

Immunoblot Analysis of 4-Hydroxynonenal—10 female wild type and *FK506-BP2* flies of indicated ages and conditions where homogenized in 150 μl of 2× sample buffer (100 mM Tris, pH 6.8, 20% glycerol, 4% SDS) containing 10% β-mercaptoethanol. Extracts were boiled for 10 min and cleared by centrifugation (5,000 rpm at room temperature, followed by 13,000 rpm at 4 °C). Total protein amounts were determined prior to gel loading using a Pierce 660-nm protein assay (Pierce), and SDS-PAGE was performed using 4–15% gradient gels and transferred to nitrocellulose membranes. 5 μg of protein extract was loaded per lane. The membranes were blotted with 5% milk in 1% Tween 20, TBS, pH 7.4, at room temperature for 1 h. The membranes were initially probed with primary anti-rabbit HNE polyclonal antibody (1:1000) (Alpha Diagnostics (San Antonio, TX) and secondary horse radish peroxidase-labeled goat anti-rabbit IgG antibody (1:2500) (Santa Cruz Biotechnology, Dallas, TX). All blots were subjected to hydrogen peroxide inactivation of secondary antibodies and reimmunoblotted using a mouse anti-tubulin antibody (1:30,000) (Developmental Studies Hybridoma Bank, Iowa City, IA). Immunostained proteins were visualized using ECL detection method, and band intensity was analyzed using ImageJ. Band intensity for each lane was normalized to its tubulin intensity values. The averages of normalized data were statistically analyzed by pairwise comparisons using a Student's *t* test. *p* values of <0.05 were considered statistically significant.

Detection of Drosophila RyR Oxidation—100 flies from different genotypes were frozen at −80C and homogenized in 500 μl of homogenization buffer (0.25 M sucrose, 10 mM Tris, pH 7.4, 20 mM NaF, 1 mM Na_3VO_4, and protease inhibitors; Roche). The homogenates were centrifuged for 10 min at 1000 × *g* at 4 °C. The resulting supernatant was removed and centrifuged at 115,000 rpm for 40 min at 4 °C in a TLA120.2 (Beckman Coulter, Brea, CA). The pellet was resuspended in a buffer containing 50 mM Tris, pH 7.4, 150 mM NaCl, and protease inhibitors. Proteins were precipitated using TCA, washed with acetone, and resuspended in 2× sample buffer (100 mM Tris, pH 6.8, 20% glycerol, 4% SDS) containing 10% β-mercaptoethanol and boiled for 10 min. The samples were subjected to SDS-PAGE using 7.5% Tris-HCl gels and transferred to nitrocellulose membranes. The membranes were incubated with primary guinea pig *Drosophila* anti-RyR antibody (1:1000) (a gift from Scott Robert L. Scott, Benjamin White Lab, National Institutes of Health) followed by appropriate secondary antibodies. The *Drosophila* RyR antibody was generated against the LRARA-ILRSLVPLEDLQGV peptide sequence (49). Immunostained proteins were visualized using ECL detection method. RyR channel oxidation was assessed by derivation of the carbonyl groups in the protein side chains to 2,4-dinitrophenylhydrazone (DNP-hyroazone) by reaction with DNPH using an OxyBlot™ protein oxidation detection kit (Millipore). RyR channel nitrosylation was assessed with anti-Cys-NO antibody (1:1000) (Alpha Diagnostic International, San Antonio, TX). For immunoprecipitation, the resuspended protein (see above) was further diluted (1:1) in a modified radioimmune precipitation assay buffer (50 mM Tris-HCl, pH 7.4, 0.9% NaCl, 5.0 mM NaF, 1.0 mM Na_3VO_4, 1% Triton X-100, and protease inhibitors) and incubated at 4 °C for 2 h with protein G Dynabeads previously incubated with anti-RyR antibody as described in protocol (Life Technologies). The immune complexes were eluted from the beads by adding 2× sample buffer followed by boiling for 5 min. Proteins were separated on SDS-PAGE gels (7.5% Tris-HCl gels) and transferred onto nitrocellulose membranes for 1.5 h at 350 mA. Membranes were immunoblotted normally using the *Drosophila* anti-RyR antibody (1:1000) and processed for DNPH as described above.

Wall Climbing/Negative Geotaxis—Virgin flies of appropriate age and genotypes were anesthetized under carbon dioxide and allowed to recover for 60 min. Empty polystyrene vials were vertically joined by tape facing each other. For the lower vial a vertical distance of 8 cm was measured above the bottom surface and marked. 10–15 flies were transferred into the lower vial. The flies were gently tapped to the bottom and the number of flies that climbed above the 8-cm mark by 10 s after the tap was counted manually.

CM9 Microscopy—CM9 muscles from 7-day-old female flies of indicated genotypes were processed for immunofluorescent microscopy using the primary antibody to Discs-large (1:500; Developmental Studies Hybridoma Bank) as previously described (35). CM9 muscle fibers were manually counted. For the analysis of myonuclei density, images were captured at 63 ×

1.6 magnification. Myonuclei were manually counted and normalized to the length of muscle fibers.

CM9 NMJ Electrophysiology—Female flies of indicated age and genotype were dissected and recorded as previously described (36).

Author Contributions—T. K.-P. was responsible for experimental design, data acquisition and interpretation, and manuscript preparation. J. A. was responsible for data acquisition and interpretation. R. E. M. was responsible for data acquisition and interpretation. B. A. E. was responsible for experimental design, data acquisition and interpretation, and manuscript preparation.

Acknowledgments—We acknowledge the Drosophila Aging Core of the Nathan Shock Center of Excellence in the Biology of Aging (which is supported in part by NIA, National Institutes of Health Grant P30-AG-013283) and the Bloomington Drosophila Stock Center (which is supported in part by National Institutes of Health Grant P40OD018537) for providing resources. Select immune reagents were also obtained from the Developmental Studies Hybridoma Bank, created by the NICHD, National Institutes of Health, and maintained at the University of Iowa Department of Biology.

References

1. Harman, D. (1956) Aging: a theory based on free radical and radiation chemistry. *J. Gerontol.* **11,** 298–300
2. Harman, D. (2006) Free radical theory of aging: an update: increasing the functional life span. *Ann. N.Y. Acad. Sci.* **1067,** 10–21
3. Gems, D., and Doonan, R. (2009) Antioxidant defense and aging in *C. elegans*: is the oxidative damage theory of aging wrong? *Cell Cycle.* **8,** 1681–1687
4. Pérez, V. I., Bokov, A., Van Remmen, H., Mele, J., Ran, Q., Ikeno, Y., and Richardson, A. (2009) Is the oxidative stress theory of aging dead? *Biochim. Biophys. Acta* **1790,** 1005–1014
5. Andziak, B., O'Connor, T. P., and Buffenstein, R. (2005) Antioxidants do not explain the disparate longevity between mice and the longest-living rodent, the naked mole-rat. *Mech. Ageing Dev.* **126,** 1206–1212
6. Duttaroy, A., Paul, A., Kundu, M., and Belton, A. (2003) A Sod2 null mutation confers severely reduced adult life span in *Drosophila*. *Genetics* **165,** 2295–2299
7. Kirby, K., Hu, J., Hilliker, A. J., and Phillips, J. P. (2002) RNA interference-mediated silencing of Sod2 in *Drosophila* leads to early adult-onset mortality and elevated endogenous oxidative stress. *Proc. Natl. Acad. Sci. U.S.A.* **99,** 16162–16167
8. Jang, Y. C., Lustgarten, M. S., Liu, Y., Muller, F. L., Bhattacharya, A., Liang, H., Salmon, A. B., Brooks, S. V., Larkin, L., Hayworth, C. R., Richardson, A., and Van Remmen, H. (2010) Increased superoxide *in vivo* accelerates age-associated muscle atrophy through mitochondrial dysfunction and neuromuscular junction degeneration. *FASEB J.* **24,** 1376–1390
9. Van Raamsdonk, J. M., and Hekimi, S. (2012) Superoxide dismutase is dispensable for normal animal lifespan. *Proc. Natl. Acad. Sci. U.S.A.* **109,** 5785–5790
10. Doonan, R., McElwee, J. J., Matthijssens, F., Walker, G. A., Houthoofd, K., Back, P., Matscheski, A., Vanfleteren, J. R., and Gems, D. (2008) Against the oxidative damage theory of aging: superoxide dismutases protect against oxidative stress but have little or no effect on life span in *Caenorhabditis elegans*. *Genes Dev.* **22,** 3236–3241
11. Edrey, Y. H., and Salmon, A. B. (2014) Free radical biology and medicine. *Free Rad. Biol. Med.* **71,** 368–378
12. Miller, R. A., Harrison, D. E., Astle, C. M., Baur, J. A., Boyd, A. R., de Cabo, R., Fernandez, E., Flurkey, K., Javors, M. A., Nelson, J. F., Orihuela, C. J., Pletcher, S., Sharp, Z. D., Sinclair, D., Starnes, J. W., *et al.* (2011) Rapamycin, but not resveratrol or simvastatin, extends life span of genetically heterogeneous mice. *J. Gerontol. A Biol. Sci. Med. Sci.* **66,** 191–201
13. Magwere, T., West, M., Riyahi, K., Murphy, M. P., Smith, R. A., and Partridge, L. (2006) The effects of exogenous antioxidants on lifespan and oxidative stress resistance in *Drosophila melanogaster*. *Mech. Ageing Dev.* **127,** 356–370
14. Bass, T. M., Weinkove, D., Houthoofd, K., Gems, D., and Partridge, L. (2007) Effects of resveratrol on lifespan in *Drosophila melanogaster* and *Caenorhabditis elegans*. *Mech. Ageing Dev.* **128,** 546–552
15. Orr, W. C., and Sohal, R. S. (1993) Effects of Cu-Zn superoxide dismutase overexpression of life span and resistance to oxidative stress in transgenic *Drosophila melanogaster*. *Arch. Biochem. Biophys.* **301,** 34–40
16. Wood, J. G., Rogina, B., Lavu, S., Howitz, K., Helfand, S. L., Tatar, M., and Sinclair, D. (2004) Sirtuin activators mimic caloric restriction and delay ageing in metazoans. *Nature* **430,** 686–689
17. Brown-Borg, H. M., and Rakoczy, S. G. (2000) Catalase expression in delayed and premature aging mouse models. *Exp. Gerontol.* **35,** 199–212
18. Canistro, D., Boccia, C., Falconi, R., Bonamassa, B., Valgimigli, L., Vivarelli, F., Soleti, A., Genova, M. L., Lenaz, G., Sapone, A., Zaccanti, F., Abdel-Rahman, S. Z., and Paolini, M. (2015) Redox-based flagging of the global network of oxidative stress greatly promotes longevity. *J. Gerontol. A Biol. Sci. Med. Sci.* **70,** 936–943
19. Parkes, T. L., Elia, A. J., Dickinson, D., Hilliker, A. J., Phillips, J. P., and Boulianne, G. L. (1998) Extension of *Drosophila* lifespan by overexpression of human SOD1 in motorneurons. *Nat. Genet.* **19,** 171–174
20. Valenzano, D. R., Terzibasi, E., Genade, T., Cattaneo, A., Domenici, L., and Cellerino, A. (2006) Resveratrol prolongs lifespan and retards the onset of age-related markers in a short-lived vertebrate. *Curr. Biol.* **16,** 296–300
21. Krivoruchko, A., and Storey, K. B. (2010) Forever young: mechanisms of natural anoxia tolerance and potential links to longevity. *Oxid. Med. Cell Longev.* **3,** 186–198
22. Lewis, K. N., Andziak, B., Yang, T., and Buffenstein, R. (2013) The naked mole-rat response to oxidative stress: just deal with it. *Antioxid. Redox. Signal.* **19,** 1388–1399
23. Parker, J. D., Parker, K. M., Sohal, B. H., Sohal, R. S., and Keller, L. (2004) Decreased expression of Cu-Zn superoxide dismutase 1 in ants with extreme lifespan. *Proc. Natl. Acad. Sci. U.S.A.* **101,** 3486–3489
24. Montgomery, M. K., Buttemer, W. A., and Hulbert, A. J. (2012) Does the oxidative stress theory of aging explain longevity differences in birds? II. Antioxidant systems and oxidative damage. *Exp. Gerontol.* **47,** 211–222
25. Brunet-Rossinni, A. K. (2004) Reduced free-radical production and extreme longevity in the little brown bat (*Myotis lucifugus*) versus two non-flying mammals. *Mech. Ageing Dev.* **125,** 11–20
26. Yan, L.-J. (2014) Positive oxidative stress in aging and aging-related disease tolerance. *Redox Biol.* **2,** 165–169
27. Epel, E. S., and Lithgow, G. J. (2014) Stress biology and aging mechanisms: toward understanding the deep connection between adaptation to stress and longevity. *J. Gerontol. A Biol. Sci. Med. Sci.* **69,** S10–S16
28. Andersson, D. C., Betzenhauser, M. J., Reiken, S., Meli, A. C., Umanskaya, A., Xie, W., Shiomi, T., Zalk, R., Lacampagne, A., and Marks, A. R. (2011) Ryanodine receptor oxidation causes intracellular calcium leak and muscle weakness in aging. *Cell Metab.* **14,** 196–207
29. Bellinger, A. M., Reiken, S., Dura, M., Murphy, P. W., Deng, S. X., Landry, D. W., Nieman, D., Lehnart, S. E., Samaru, M., LaCampagne, A., and Marks, A. R. (2008) Remodeling of ryanodine receptor complex causes "leaky" channels: a molecular mechanism for decreased exercise capacity. *Proc. Natl. Acad. Sci. U.S.A.* **105,** 2198–2202
30. Ondrias, K., Marx, S. O., Gaburjakova, M., and Marks, A. R. (1998) FKBP12 modulates gating of the ryanodine receptor/calcium release channel. *Ann. N.Y. Acad. Sci.* **853,** 149–156
31. Lehnart, S. E., Terrenoire, C., Reiken, S., Wehrens, X. H., Song, L. S., Tillman, E. J., Mancarella, S., Coromilas, J., Lederer, W. J., Kass, R. S., and Marks, A. R. (2006) Stabilization of cardiac ryanodine receptor prevents intracellular calcium leak and arrhythmias. *Proc. Natl. Acad. Sci. U.S.A.* **103,** 7906–7910
32. Gaburjakova, M., Gaburjakova, J., Reiken, S., Huang, F., Marx, S. O., Rosemblit, N., and Marks, A. R. (2001) FKBP12 binding modulates ryanodine receptor channel gating. *J. Biol. Chem.* **276,** 16931–16935
33. Mei, Y., Xu, L., Kramer, H. F., Tomberlin, G. H., Townsend, C., and Meissner, G. (2013) Stabilization of the skeletal muscle ryanodine receptor ion

channel-FKBP12 complex by the 1,4-benzothiazepine derivative S107. *PLoS One* **8,** e54208
34. Siegel, M. P., Kruse, S. E., Percival, J. M., Goh, J., White, C. C., Hopkins, H. C., Kavanagh, T. J., Szeto, H. H., Rabinovitch, P. S., and Marcinek, D. J. (2013) Mitochondrial-targeted peptide rapidly improves mitochondrial energetics and skeletal muscle performance in aged mice. *Aging Cell* **12,** 763–771
35. Rawson, J. M., Kreko, T., Davison, H., Mahoney, R., Bokov, A., Chang, L., Gelfond, J., Macleod, G. T., and Eaton, B. A. (2012) Effects of diet on synaptic vesicle release in dynactin complex mutants: a mechanism for improved vitality during motor disease. *Aging Cell* **11,** 418–427
36. Mahoney, R. E., Rawson, J. M., and Eaton, B. A. (2014) An age-dependent change in the set point of synaptic homeostasis. *J. Neurosci.* **34,** 2111–2119
37. Gordon, M. D., and Scott, K. (2009) Motor control in a *Drosophila* taste circuit. *Neuron* **61,** 373–384
38. Tong, M., and Jiang, Y. (2015) FK506-binding proteins and their diverse functions. *Curr. Mol. Pharmacol.* **9,** 48–65
39. Zheng, J., Mutcherson, R., 2nd, and Helfand, S. L. (2005) Calorie restriction delays lipid oxidative damage in *Drosophila melanogaster*. *Aging Cell* **4,** 209–216
40. Toroser, D., Orr, W. C., and Sohal, R. S. (2007) Carbonylation of mitochondrial proteins in *Drosophila melanogaster* during aging. *Biochem. Biophys. Res. Commun.* **363,** 418–424
41. Castello, P. R., Drechsel, D. A., and Patel, M. (2007) Mitochondria are a major source of paraquat-induced reactive oxygen species production in the brain. *J. Biol. Chem.* **282,** 14186–14193
42. Umanskaya, A., Santulli, G., Xie, W., Andersson, D. C., Reiken, S. R., and Marks, A. R. (2014) Genetically enhancing mitochondrial antioxidant activity improves muscle function in aging. *Proc. Natl. Acad. Sci. U.S.A.* **111,** 15250–15255
43. Haas, J., Frese, K. S., Peil, B., Kloos, W., Keller, A., Nietsch, R., Feng, Z., Müller, S., Kayvanpour, E., Vogel, B., Sedaghat-Hamedani, F., Lim, W. K., Zhao, X., Fradkin, D., Köhler, D., *et al.* (2015) Atlas of the clinical genetics of human dilated cardiomyopathy. *Eur. Heart J.* **36,** 1123–1135a
44. Wu, S., Ibarra, M. C., Malicdan, M. C., Murayama, K., Ichihara, Y., Kikuchi, H., Nonaka, I., Noguchi, S., Hayashi, Y. K., and Nishino, I. (2006) Central core disease is due to RYR1 mutations in more than 90% of patients. *Brain* **129,** 1470–1480
45. Betzenhauser, M. J., and Marks, A. R. (2010) Ryanodine receptor channelopathies. *Pflugers Arch.* **460,** 467–480
46. Wehrens, X. H., Lehnart, S. E., Huang, F., Vest, J. A., Reiken, S. R., Mohler, P. J., Sun, J., Guatimosim, S., Song, L. S., Rosemblit, N., D'Armiento, J. M., Napolitano, C., Memmi, M., Priori, S. G., Lederer, W. J., *et al.* (2003) FKBP12.6 deficiency and defective calcium release channel (ryanodine receptor) function linked to exercise-induced sudden cardiac death. *Cell* **113,** 829–840
47. Grimes, K. M., Reddy, A. K., Lindsey, M. L., and Buffenstein, R. (2014) And the beat goes on: maintained cardiovascular function during aging in the longest-lived rodent, the naked mole-rat. *Am. J. Physiol. Heart Circ. Physiol.* **307,** H284–H291
48. Wang, T., Donahoe, P. K., and Zervos, A. S. (1994) Specific interaction of type I receptors of the TGF-beta family with the immunophilin FKBP-12. *Science* **265,** 674–676
49. Gao, S., Sandstrom, D. J., Smith, H. E., High, B., Marsh, J. W., and Nash, H. A. (2013) *Drosophila* ryanodine receptors mediate general anesthesia by halothane. *Anesthesiology* **118,** 587–601